UDC 004.932:519.6:620.179.13 DOI: https://doi.org/10.37434/tdnk2025.02.03

APPLICATION OF WAVELET ANALYSIS AND DIFFERENTIAL-INTEGRAL GRAPHICAL METHODS FOR THERMOGRAMS PROCESSING IN THERMAL NONDESTRUCTIVE TESTING

V.O. Storozhenko, O.V. Miahkyi, S.M. Meshkov, R.P. Orel

RTC «Thermocontrol» of Kharkiv National University of Radio Electronics. 14 Nauky Ave., 61166, Kharkiv, Ukraine. E-mail: roman.orel@nure.ua

The problem of increasing the informativeness and reliability of the results of non-destructive testing of high-tech objects of complex structures by the active thermal method is considered. To solve this, we suggest combining the developed integral-differential signal processing method with existing information processing methods based on the formalization of the description of temperature fields. The stages of this transformation are considered: the formation of an operator that characterizes the temperature field that arises on the surface of the control object due to the action of thermal influence and boundary conditions associated with its state and structure. The relations between the stages were analyzed, based on which obstacles and noises were identified that might arise at each of them and thus limit the informativeness and probability of detecting continuity violations. The following sources of interference were considered: non-uniform heating of the surface of the control object and non-uniformity of the adhesive layer under the honeycomb structure cladding. A set of methods for reducing the impact of these interferences is proposed, including wavelet analysis, joint and differential filtering methods, integral analysis methods, decision-making criteria, and classical image processing methods adapted to the infrared range. It has been shown that the use of these methods reduces the interference level to 0.6 °C (instead of 2 °C). The temperature contrast caused by the different thicknesses of the adhesive layer can be reduced to 0.4 °C (instead of 1.2 °C). Statistics obtained during thermal non-destructive testing of a batch of honeycomb samples showed that the probability of detecting suprathreshold defects can reach 90%. 9 Ref., 3 Fig.

Keywords: thermal control, composite structures, interference, wavelet, image processing, method sensitivity

Introduction. The thermal method is widely used for non-destructive testing of critical industrial products, such as complex honeycomb structures used in aerospace engineering. A thermal non-destructive testing (TNDT) system usually consists of a heater (source of thermal excitation), a device for scanning the surface of the test object (TC), and a thermal imager (recording device) [1]. Hidden defects in the TC (for example, cracks and voids) are detected on the thermogram obtained with a thermal imager as local areas with increased or decreased temperature. A useful signal from the defect is the local temperature contrast ΔT. However, such areas also arise for other reasons not related to defects. This may be uneven heating along the surface of the TC, its structural inhomogeneities, etc. As a result, interference occurs that reduces the sensitivity of TNDT systems and the probability of detecting defects.

Problem statement. In the process of TNDT, obstacles arise both in the control object itself and in the environment, and in the recording equipment. Interference can be added to the true temperature signal T (additive interference $\tilde{A}$) or multiply with it (multiplicative interference $\tilde{M}$) [2]:

$$u(x,y,\tau)=\tilde{M}T(x,y,\tau)+\tilde{A}.$$

It is obvious that the registered signal $u \equiv T$ only if $\tilde{M} \equiv 1$ and $\tilde{A} \equiv 0$.

The best TNDT procedure is one in which the sensitivity of the method is limited by the radiation detector, i.e. $\tilde{M} \equiv 1$ and $\tilde{A} \to \min$. The limiting value of the registered signal is the passport temperature sensitivity of the thermal imager ΔT_{res}, which reaches in modern models 0.01 °C.

Further improvement of temperature resolution is possible by using the accumulation method [3–5]. However, in natural conditions, air convection and external emitters create noise at approximately 0.1 °C, which can be considered the temperature sensitivity limit of TNDTs in real conditions [6]. Each type of noise can be described in terms of temperature. There are structural $\sqrt{\Delta\overline{T}^2_{str}}$, hardware $\sqrt{\Delta\overline{T}^2_{app}}$ and external noise. Using these terms for uncorrelated noise, the signal-to-noise ratio can be determined as [7]:

$$S=\frac{\Delta T_{\tau}}{\sqrt{\left(\Delta T_{res}\right)^2+\left(\Delta T_{str}\right)^2+\left(\Delta T_{ext}\right)^2}},$$

V.O. Storozhenko – https://orcid.org/0000-0002-7609-2955, O.V. Miahkyi – https://orcid.org/0000-0002-0442-5570.
S.M. Meshkov – https://orcid.org/0000-0003-3464-8318, R.P. Orel – https://orcid.org/0000-0002-3592-2393

where ΔT_{res} – hardware noise; ΔT_{str} – structural noise; ΔT_{ext} – external noise.

When using time parameters, the equivalent time noise can be estimated by the expression [3–5]:

$$\Delta T_{\tau} = \frac{\partial T(\tau)}{\partial \tau}\Delta\tau .$$

External noise is created by the heat flux from surrounding objects, either reflected from the object under inspection or directly entering the thermal imager. Sources of this noise are heaters, the sun, heaters, electric lighting lamps, etc. Direct radiation is eliminated using hoods, screens, filters, etc. The most difficult to eliminate is radiation reflected from the object under inspection. In an active TC, the main source of external noise is the heater. For example, during the optical heating of metals, residual lamp radiation can seriously distort the appearance of thermograms and lead to incorrect estimates of defect parameters if only temperature models of thermal defectometry are used. Therefore, the development of methods for combating interference characteristics of TNDTs and means of increasing the level of the useful signal is an urgent task.

To accomplish the task, thermograms of a honeycomb sample were used, obtained using an infrared camera IRTIS-200 with the following characteristics: spectral range of 3-5 μm, sensitivity of 0.05 °C, and spatial resolution of 2 mrad.

The selected class of TC is characterized by such sources of interference as non-uniform heating of the TC surface and non-uniformity of the adhesive layer. In order to reduce the level of each of the interferences, the following methods are proposed:

- two-dimensional discrete wavelet Meyer transform and frequency filtering to reduce the level of non-uniformity of the heater thermal field;
- differential-integral graphic image processing methods to minimize the influence of interference with a characteristic differential profile such as the inhomogeneity of the adhesive layer.

Application of the wavelet analysis. The presence of interference leads to the detection of a non-existent defect, i.e. to a «false alarm», or to the failure to detect an existing defect. New opportunities for interference compensation are provided by the use of the wavelet analysis apparatus. Wavelet transforms of a one-dimensional signal consist in its expansion in terms of the basis ψ, constructed from a localized function (wavelet) and having certain properties of a localized function (wavelet) through scale changes and transfers. Each of the functions of this basis characterizes both a certain spatial (or temporal) frequency component of the signal and the localization of this component in physical space (or time) [3].

The wavelet analysis apparatus includes a large number of various wavelet transforms [4, 5], but in this work we are interested in one-dimensional and two-dimensional dyadic wavelet transforms.

It is known that a multiscale analysis algorithm has been developed for an orthonormal wavelet basis on a binary lattice [4]. The algorithm is based on the following assumptions:

- the signal space V can be partitioned into hierarchically nested subspaces V_j that do not intersect, and the union of which gives the space in the limit $L^2(\boldsymbol{R})$;
- for any function $s(t) \in V_j$, its compact version belongs to the space V_{j-1};
- there exists a function $\varphi(x) \in V_0$, for which its shifts $\varphi_{0,k} = \varphi(t-k)$, $k \in \mathbb{Z}$ form an orthonormal basis of the space V_0.

Then since the functions $\varphi_{0,k}(t)$ form an orthonormal basis of the space, the functions $\varphi_{j,k}(t) = 2^{-j/2}\varphi(2^{-j}t-k)$ also form an orthonormal basis V_0.

The scaling function $\varphi(t)$ (parent wavelet) is commonly called a scalable function because it creates by $\varphi_{j,k}(t)$ scaled versions of itself in the signal space. A signal $s(t)$ can be represented by a set of successive approximations $s_j(t)$ in subspaces V_j. The variable j is called the scale factor. The signal $s(t)$ is the approximation limit $s_j(t) \in V_j$, i.e. $s(t) = \lim\limits_{j\to\infty} s_j(t)$. Therefore, for small j values, rough approximations $s(t)$ are obtained, and for large values, more accurate ones.

Function $\psi \in L^2(\boldsymbol{R})$ is called R-function, if for this function the scaling functions $\{\psi_{jk}\}$ form a basis, which is defined by the expression:

$$\psi_{jk}(t) = 2^{-j/2}\psi(2^{-j}t-k), \quad j,k \in \mathbb{Z}, \qquad (1)$$

where – $\mathbb{Z}$ – the set of integers is a Riesz basis [3, 4].That is, for the function ψ_{jk} there are two constants A_w and B_w, for which the condition is fulfilled $0 < A_w \le B_w < \infty$, then the expression

$$A_w \left\|\{c_{jk}\}\right\|^2 \le \left\| \sum_{j\in\mathbb{Z}}\sum_{k\in\mathbb{Z}} c_{jk}\psi_{jk} \right\|^2 \le B_w \left\|\{c_{jk}\}\right\|^2$$

is a wavelet framework and holds for any (limited by a twice quadratic sum) sequence $\{c_{jk}\}$:

$$\left\|\{c_{jk}\}\right\|^2 = \sum_{j\in\mathbb{Z}}\sum_{k\in\mathbb{Z}} \left|c_{jk}\right|^2 < \infty .$$

The Riesz basis is unconditional, that is, the order of the vectors in it can be arbitrary.

Any localized R-function $\psi \in L^2(\boldsymbol{R})$ is called an R-wavelet (mother wavelet or simply a wavelet) if there exists a function $\dot{\psi} \in L^2(\boldsymbol{R})$ for it (its pair, twin) such that the families $\{\psi_{jk}\}$ and $\{\dot{\psi}_{jk}\}$, are constructed according to (1) and:

$$\dot{\psi}_{jk}(t) = 2^{-j/2}\dot{\psi}(2^{-j}t - k), \quad j,k \in \mathbb{Z},$$

are even bases of the functional space $L^2(\boldsymbol{R})$. Here $\{\dot{\psi}_{jk}\}$ – is pair of the basis $\{\psi_{jk}\}$ in the sense that the scalar multiplication of these functions satisfies the condition:

$$\langle \psi_{jk}, \dot{\psi}_{lm} \rangle = \delta_{jl}\delta_{km},$$

where δ_{jl}, δ_{km} are Kronecker symbols.

In the general case, the signal reconstruction at the *n*-th resolution level is given by the expression:

$$s(t) = \sum_{k=-\infty}^{\infty} a_{j_n,k}\varphi_{j_n,k}(t) + \sum_{j=j_n}^{\infty}\sum_{k=-\infty}^{\infty} d_{j,k}\psi_k(t), \quad (2)$$

where $a_{j_n,k}$ and $d_{j,k}$ – approximating and detailing coefficients at the n-th level of decomposition, respectively. They are determined by the ratios:

$$a_{j_n,k} = \int_{-\infty}^{\infty} s(t)\varphi_{j_n,k}(t)dt, \; d_{j,k} = \int_{-\infty}^{\infty} s(t)\psi_{j,k}(t)dt. \quad (3)$$

The wavelet $\psi(t)$ determines the fine structure of the analyzed signal, and the scaling function $\varphi(t)$ is responsible for its coarse approximation [3, 6, 7].

The pair of relations (2) and (3) defines the one-dimensional dyadic wavelet transform.

In the case of a two-dimensional dyadic wavelet transform, the one-dimensional signal under investigation $s(t)$ is replaced by a function of two variables $s(x,y)$, of which an image is a special case.

Then the wavelet basis also becomes a function of two variables:

$$\psi_{j,k}(V) = 2^{-j/2}\psi(2^{-j}V - k),$$
$$\varphi_{j,k}(V) = 2^{-j/2}\varphi(2^{-j}V - k), \quad (4)$$

where $V(x,y) \in L^2$, $(j,k) \in L^2$.

Thus, for image processing, it is better to use the two-dimensional dyadic Meyer wavelet transform, which is defined by relations (2) and (3) using relations (4).

A raster image is a discrete signal to which two-dimensional discrete wavelet transforms can be applied. The proposed idea of combating interference in TNDT by wavelet image processing is as follows. First, using a direct two-dimensional dyadic wavelet transform, we decompose the original image using the maximum possible number of decomposition levels. Then we equate all approximating and detailing coefficients at this maximum decomposition level to zero and restore the image using an inverse two-dimensional dyadic wavelet transform. The described transformations were tested on an infrared image using the discrete Meyer wavelet, resulting in a significantly corrected spatial distribution of the thermal field (Fig. 1). The proposed algorithm implements the application of a low spatial frequency filter to the original image and removes thermal field variations with the largest spatial scales [6]. This does not lead to a loss of information about defects, since their characteristic spatial scales are usually smaller. The criterion for selecting a wavelet transform from a large number of wavelets was the features of the geometry of the thermal field created by the heater [8]. Taking into account the properties of the sample thermogram, a discrete Meyer wavelet was selected. In this case, it is quite smooth, and therefore was used in these studies. The result of the processing is shown in Fig. 1. To further reduce the level of interference, other processing methods must be used.

The resulting contrast image (Fig. 1, *c*) allows us to identify areas with probable locations of defects, but their precise determination requires the use of additional methods of modern image processing equipment.

Using differential-integral graphic methods of image processing. Along with wavelet transforms, additional filtering methods were used to increase the reliability of control results. To eliminate certain types of interference caused by the heterogeneity of the cellular panel structure, a number of additional joint filtering methods were used. The combined approach

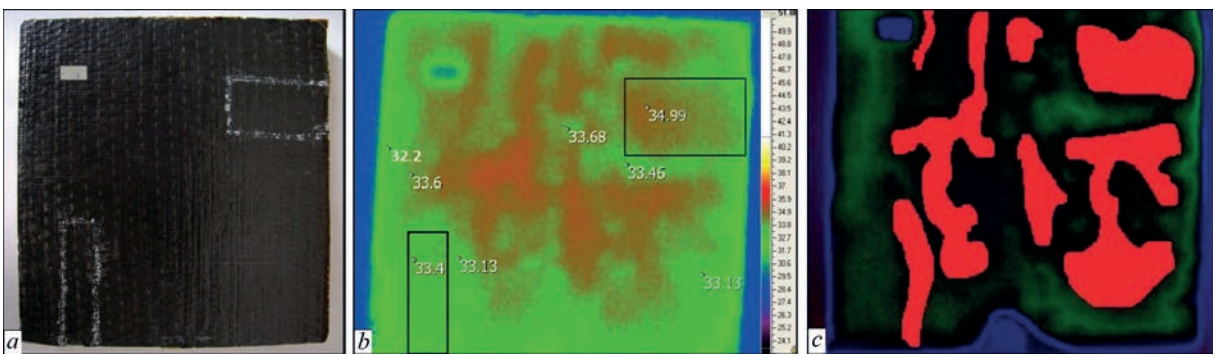

Fig. 1. Thermogram processing: *a* – visible image of a sample of a honeycomb panel (CB Yuzhnoye) with carbon fiber skins and paper filler with hidden defects of the «not glued» type; *b* – thermogram; *c* – corrected spatial distribution of the thermal field

significantly increased the reliability of the TNDT method. If the reliability of the developed method is considered as the probability of correct processing of results, then it is formed as the inverse probability of the total probability of two erroneous decisions [6]:

$$P^* = 1 - (P_1 + P_2)/2, \qquad (5)$$

To increase the capacity and effectiveness of point estimates of risks of the first and second kind, which also reflect the probabilities of these erroneous decisions, it is necessary to conduct multiple experiments to check clearly non-defective and clearly defective samples [9].

It is known that the statistical probability of a defect detection event is equal to the ratio of the number of favorable outcomes to the total number of possible outcomes [9]:

$$P(A) = \frac{m}{n},$$

where $P(A)$ is probability of an event A; m – number of favorable outcomes to event A; n – total number of possible outcomes. From this it can be seen that the more accurate each individual measurement, the more accurate the entire control, therefore it is advisable to use an additional method of differential filtering.

To eliminate the second type of interference caused by the non-uniformity of the adhesive layer, it is proposed to use the differential filtration method [7]. It is known that the thickness of the adhesive layer between the honeycombs and the shell is non-uniform. It has been established that the different thickness of the adhesive layer is equivalent to a change in thermal resistance and leads to the appearance of temperature contrasts on the surface of the TC. Analysis of the obtained experimental data showed that these contrasts differ from the useful signal (ΔT caused by a defect) time dependence $\Delta T(\tau)$. This fact was used to construct a method for suppressing this interference by computer processing of thermograms, based on obtaining the derivative $\partial T/\partial\tau$ as a function of the coordinate x for the interference and for the defect containing the TC (Fig. 2).

According to Fig. 2, after processing, the difference between these functions is easily noticeable in the nature of the behavior of the partial derivative of the function F, which for the signal has a positive value in the first phase and a negative value in the second, which for the noise has the opposite value in the corresponding phases. This is the basis of the method. Signals, the partial derivative of which corresponds to noise, are filtered.

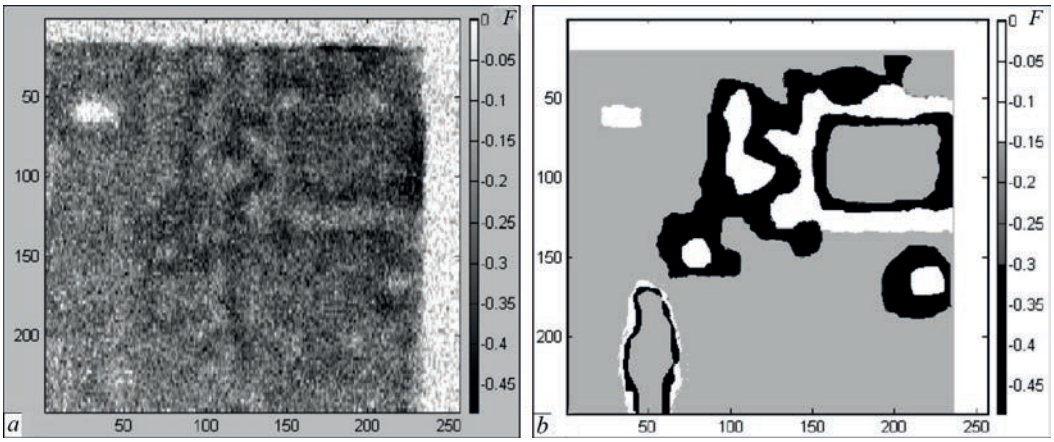

Fig. 2. Image of the two-dimensional dependence of the partial derivative F over time on the coordinates x and y for the original image (*a*) and after processing (*b*)

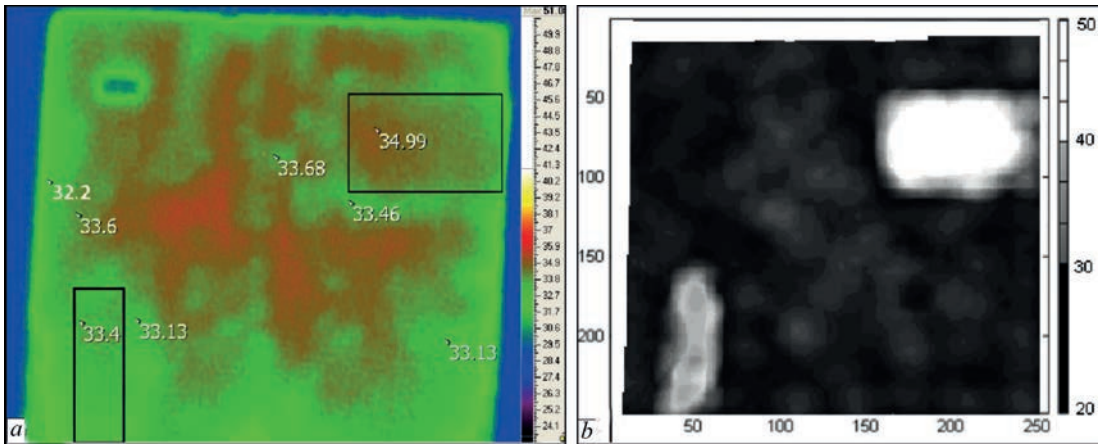

Fig. 3. The result of the final processing of the thermogram of the sample: *a* – initial thermogram; *b* – thermogram after processing with detected defects

The essence of the method is to calculate a two-dimensional operator, the elements of which are the corresponding partial derivatives with respect to time [5]:

$$F_{i,j} = \frac{\partial T'_{i,j}(x,y)}{\partial t},$$

where $T'_{i,j}(x,y)$ is element of the operator of corrected temperatures; i, j – integers, corresponding pixel numbers in x and y; $F_{i,j}$ – element of the characteristic operator.

After calculating the operator (5), the thermogram recovery procedure is carried out, but without signals responsible for a certain interference. The processed thermogram takes the form shown in Fig. 3, *b*. Comparison of this thermogram with the original (Fig. 3, *a*) confirms the fact that the reliability of detecting defects (shown by light spots) has significantly increased after processing [9]. At the same time, the interference level due to the different thickness of the layers of multilayer objects is reduced from 1.2 to 0.4 °C.

Conclusions

Experiments have shown that the use of discrete Meyer wavelet transforms in processing the results of TNDT of a honeycomb panel allowed to reduce the level of interference caused by uneven heating by 2 times from 1.4 to 0.7 °C. This transformation in combination with differential-integral methods allows to significantly increase the sensitivity of the method to detect defects such as «delamination» and «ungluing» in honeycomb structures and other multilayer compositions. As for the interference caused by the inhomogeneity of the emissivity, it was possible to reduce it to 0.6 °C (instead of 2 °C), and the temperature contrast caused by the different thickness of the adhesive layer was reduced to 0.4 °C (instead of 1.2 °C). Statistics obtained during TNDT of a batch of cellular samples showed that the probability of detecting suprathreshold defects can reach 90%.

The use of the above methods creates all the prerequisites for moving from an individual method of defect identification in production to an automated one based on appropriate technical means.

References

1. Storozhenko, V.A., Maslova, V.A. (2004) *Thermography in diagnostics and nondestructive testing*. Kharkov: Smith [in Russian].
2. Maldague, Xavier P.V. (2001) *Theory and practice of infrared technology for nondestructive testing*. John Wiley & Sons, Inc.
3. Miahkyi, A.V., Lazorenko, O.V., Storozhenko, V.A. (2013) Processing the results of thermal defectoscopy of honeycomb structures in order to reduce the level of obstacle. *Visnik NTU «HPI», serija «Elektroenergetika ta peretvorjuval'na tehnika»*, **34**, 108–122 [in Russian].
4. Chernogor, L.F., Lazorenko, O.V., Potapov, A.A. (2012) Wavelet analysis of model fractal ultra-wideband signals. *Proceeding of 6th International Conference on Ultrawideband and Ultrashort Impulse Signals,* Sevastopol, Ukraine, 291–293. DOI: https://doi.org/10.1109/UWBUSIS.2012.6379809
5. Bathe, K.J., Wilson, E.L. (1976) *Numerical methods in finite element analysis*. Prentice-Hall, Englewood Cliffs, N.J.
6. Storozhenko, V., Orel, R., Miahkyi, A. (2016) Optimization of the procedure of thermal flaw detection of the honeycomb constructions by improving the accuracy of interference function. *Eastern-European J. of Enterprise Technologies*, 5(**5**), 12–18. DOI: https://doi.org/10.15587/1729-4061.2016.79563
7. Mallat, S.A. (2008) *Wavelet tour of signal processing*. The Sparse Way, Academic Press, N.Y.
8. Lazorenko, O.V., Chernogor, L.F. (2009) *Ultra-wideband signals and processes*. Kharkiv: V.N. Karazin Kharkiv National University [in Russian].
9. Storozhenko, V.O., Meshkov, S.M., Orel, R.P., Miahkyi, O.V. (2022) Reducing the level of interference at thermal non-destructive testing considering the specific thermal physical and morphological characteristics of the object. *Tekh. Diahnost. ta Neruiniv. Kontrol*, **4**, 47–51 [in Ukrainian]. DOI: https://doi.org/10.37434/tdnk2022.04.04

ВИКОРИСТАННЯ ВЕЙВЛЕТ-АНАЛІЗУ ТА ДИФЕРЕНЦІАЛЬНО-ІНТЕГРАЛЬНИХ ГРАФІЧНИХ МЕТОДІВ ДЛЯ ОБРОБКИ ТЕРМОГРАМ У ТЕПЛОВОМУ НЕРУЙНІВНОМУ КОНТРОЛІ

В.О. Стороженко, О.В. Мягкий, С.М. Мешков, Р.П. Орел

НТЦ «Термоконтроль» Харківського національного університету радіоелектроніки. 61166, м. Харків, пр. Науки, 14.
E-mail: roman.orel@nure.ua

Розглянуто проблему підвищення інформативності та достовірності результатів неруйнівного контролю високотехнологічних об'єктів складної структури активним тепловим методом. Для її вирішення запропоновано використовувати комбінації розроблених інтегрально-диференціальних методів обробки сигналів у сукупності з існуючими методами обробки інформації, заснованими на формалізації опису температурних полів. Розглянуто етапи цього перетворення: формування оператора, який характеризує температурне поле, що виникає на поверхні об'єкта контролю внаслідок дії теплового впливу та граничних умов, пов'язаних з його станом та структурою. Проаналізовано зв'язки між етапами, на підставі чого виявлено перешкоди та шуми, які можуть виникати на кожному з них і таким чином обмежувати інформативність і вірогідність виявлення порушень суцільності. Для розгляду прийняті такі джерела перешкод, як неоднорідність нагрівання поверхні об'єкта контролю та неоднорідність клейового шару під обшивкою сотової структури. Запропоновано комплекс методів зниження впливу цих перешкод, серед яких вейвлет-аналіз, методи спільної та диференціальної фільтрації, інтегральні методи аналізу, критерії прийняття рішень і класичні методи обробки зображень, які адаптовано до інфрачервоного діапазону. Показано, що застосування вказаних методів знижує рівень перешкоди до 0,6 °С (замість 2 °С). Температурний контраст, викликаний різнотовщинністю клейового шару, вдається зменшити до 0,4 °С (замість 1,2 °С). Статистика, яка отримана при проведенні теплового неруйнівного контролю партії сотових зразків, показала, що вірогідність виявлення надпорогових дефектів може досягати 90%. Бібліогр. 9, рис. 3.

Ключові слова: тепловий контроль, композиційні структури, перешкоди, вейвлет, обробка зображень, чутливість методу

Отримано 29.03.25
Отримано у переглянутому вигляді 18.04.25
Прийнято 12.05.25